Archives of Biochemistry and Biophysics 479 (2008) 153–157

Contents lists available at ScienceDirect

Archives of Biochemistry and Biophysics

journal homepage: www.elsevier.com/locate/yabbi

Mapping the putative binding site for uPA protein in Esophageal Cancer-Related Gene 2 by heteronuclear NMR method

Yong Geng [a], Yingang Feng [a], Tao Xie [a], Yuanyuan Dai [b], Jinfeng Wang [a,*], Shih-Hsin Lu [c]

[a] National Laboratory of Biomacromolecules, Institute of Biophysics, Chinese Academy of Sciences, 15 Datun Road, Beijing 100101, China
[b] Department of Clinical Pharmacology, Cancer Institute, Peking Union Medical College and Chinese Academy of Medical Sciences, Beijing 100021, China
[c] Department of Etiology and Carcinogenesis, Cancer Institute, Peking Union Medical College and Chinese Academy of Medical Sciences, Beijing 100021, China

ARTICLE INFO

Article history:
Received 15 July 2008
and in revised form 25 August 2008
Available online 18 September 2008

Keywords:
ECRG2
Kazal-type domain
Serine proteinase inhibitor
Urokinase-type plasminogen activator
Reactive site loops

ABSTRACT

Esophageal Cancer-Related Gene 2 (ECRG2) is a novel member of the KAZAL-type serine proteinase inhibitor family and plays an important role in the inhibition of human esophageal cancer cell proliferation. The previous studies have shown that ECRG2 can bind the urokinase-type plasminogen activator (uPA)/plasmin system and inhibit its activity. In this study, the strategy of cloning, overexpression, and purification of ECRG2 for obtaining a properly folded ECRG2 with accurately formed disulfide bonds was established. The heteronuclear NMR experiments were performed with isotope labeled ECRG2 to investigate the binding interface of the protein with uPA. The sequence regions of ECRG2 for uPA binding were determined. Analysis indicates that the uPA-binding loops of ECRG2 are in correspondence with the reactive site loops for binding of serine proteinase in turkey ovomucoid third domain (OMTKY3). The structural similarity of ECRG2 to OMTKY3 was identified and a model for ECRG2 was proposed.

Esophageal Cancer-Related Gene 2 (ECRG2,[1] GenBank Accession No.: AF268198) is down-regulated in esophageal squamous cell carcinoma (ESCC) and involved in the induction of the apoptosis in esophageal cancer cell lines [1]. Bioinformatics analysis has indicated that ECRG2 is a novel member of the KAZAL-type serine proteinase inhibitor family showing 97% sequences homologous to a KAZAL-type serine proteinase inhibitor (http://www.smart.embl-heidelberg.de). ECRG2 gene encodes a protein consisting of 85 residues. The N-terminal 1–19 residues encode a signal peptide, and the C-terminal 30–85 residues consist of a conserved Kazal-type domain with the Kazal motif ($C–X_{various}–C–X_7–C–X_6–Y–X_3–C–X_{2,3}–C–X_{17}–C$), whereas the residues 20–29 link these two regions in the protein (Fig. 1). In esophageal cancer cells, ECRG2 acts as a bifunctional protein associated with the regulation of cell proliferation and induction of apoptosis [2]. ECRG2 can interact with metallothionein 2A (MT2A) which is involved in the regulation of cell proliferation and apoptosis as well as various other physiological processes [3,4], playing an important role in the carcinogenesis of esophageal cancer [2,5]. Recently, the growing data of evidence have indicated that some members of the KAZAL-type proteinase inhibitor family may be involved in the regulation of invasion and metastasis of tumor cells. RECK (reversion-inducing cysteine-rich protein with Kazal motif) is a membrane-anchored glycoprotein that negatively regulates matrix metalloproteinases (MMPs) and inhibits tumor metastasis and angiogenesis by negatively regulating the activity of MMPs which are essential for proper extracellular matrices (ECM) remodeling [6–8]. A tumor-associated trypsin inhibitor (TATI) was found to be identical to the earlier described pancreatic secretory trypsin inhibitor (PSTI) [9], which is also called the Kazal inhibitor. The ECRG2 sequence is highly homologous to RECK and TATI (Fig. 1), suggesting the possible ability of ECRG2 for degradation of the ECM. More recent research has shown that ECRG2 can inhibit the activity of urokinase-type plasminogen activator (uPA)/plasmin system, and plays an important role in the prevention of tumor cell migration and invasion by regulation of plasmin-mediated proteolysis of the ECM [10].

The present study is aimed to explore the binding interface between ECRG2 and uPA by heteronuclear NMR experiments. Thus, the recombinant isotope labeled ECRG2 is required. However, the Kazal-type domain of ECRG2 contains conserved cysteine residues, Cys32, Cys45, Cys53, Cys64, Cys67, and Cys85, which are expected to form three pairs of disulfide bonds (Fig. 1). Here, we report the cloning, overexpression, and purification of ECRG2 which provided a properly folded protein with accurately formed disulfide bonds. The model structure of ECRG2 was obtained, and the putative binding site of uPA protein on ECRG2 was determined.

* Corresponding author. Fax: +86 10 64872026.
E-mail address: jfw@sun5.ibp.ac.cn (J. Wang).

[1] *Abbreviations used:* ECRG2, Esophageal Cancer-Related Gene 2; ESCC, esophageal squamous cell carcinoma; MT2A, metallothionein 2A; MMPs, matrix metalloproteinases; ECM, extracellular matrices; TATI, tumor-associated trypsin inhibitor; PSTI, pancreatic secretory trypsin inhibitor; uPA, urokinase-type plasminogen activator.

0003-9861/$ - see front matter © 2008 Elsevier Inc. All rights reserved.
doi:10.1016/j.abb.2008.08.023

Fig. 1. Sequence alignment of human ECRG2 with RECK from human fibroblast, TATI from urine of a patient with ovarian cancer, and OMTKY3 from turkey egg white. The disulfide bridges between conserved cysteine residues in the Kazal domain of the sequences are indicated.

Materials and methods

Cloning, overexpression, and purification of ECRG2

Analysis of ECRG2 sequence has indicated that the segment of the N-terminal 19 residues behaviors as a trans-membrane peptide. For obtaining the recombinant ECRG2 protein, these 19 amino acids were truncated in the construction of the expression vector. Thus, peptide ECRG2(20–85) (called as ECRG2 hereafter), was expressed and purified for present study.

A DNA fragment encoding ECRG2 was amplified by PCR using the forward primer (cgcgggggaattcattgagggtcgctcagaagctgctagtctgtctcca) and backward primer (aaagaagtgctaccttcaacgattttcgagcggggc) which introduce an EcoRI site and a sequence encoding a factor Xa cleavage site at the 5′ end and a HindIII site at the 3′ end of the gene, respectively. The fragment was inserted into the T7 RNA polymerase-based expression vector pET-32a. Another DNA fragment encoding a linker peptide (SGSGSGSGSG) including EcoRI and EcoRV sites was synthesized and inserted into the vector pET-32a. The resulting expression vector (Supplementary material (SM) Fig. 1) for thioredoxin (Trx) fusion protein ECRG2, namely pET-32a-Trx-(linker-Xa)-ECRG2, was used for the expression and purification of ECRG2.

The pET-32a-Trx-(linker-Xa)-ECRG2 plasmid was transformed into the oxidative cytoplasm of *Escherichia coli* Origami (DE3) strain. The *E. coli* Origami (DE3)/pET-32a-Trx-(linker-Xa)-ECRG2 strain was grown overnight in 100 ml LB media (with 50 μg/ml ampicillin and 15 μg/ml kanamycin) at 37 °C. The overnight culture was used to inoculate another 1000 ml LB media. When the culture OD_{600} reached 0.6, the fusion protein expression was initiated by adding IPTG to a final concentration of 1 mM. After 20 h of additional cultivation at 16 °C, cells were harvested by centrifugation at 4000 rpm for 30 min. The cell was then resuspended in 20 ml of buffer A (50 mM Tris/HCl, pH 8.0, 300 mM NaCl, 10 mM imidazole) with 0.5 mM PMSF, 0.2 mg/ml lysozyme, 0.2 mg/ml DNaseI, and 2 mg/ml benzamidine. The cells were lysed by three 30 s sonication steps at 4 °C (Labsonic U sonicator at 150 W intensity) followed by overnight freezing at −80 °C. After thawing, the extract was centrifuged for 60 min at 40,000 rpm and 4 °C to separate the soluble and insoluble portions.

The soluble fusion protein Trx-(linker-Xa)-ECRG2 was purified using a metal-chelating affinity chromatography. For this, the supernatant was collected and loaded onto a Ni^{2+}-chelating column (10 ml) pre-equilibrated with buffer A. The column was extensively washed first with the buffer A, followed by buffer A containing 10 mM imidazole, and finally with factor Xa buffer (50 mM Tris–HCl, pH 8.0, 140 mM NaCl, 5 mM $CaCl_2$). Then the factor Xa (1 U/mg of Trx-Xa-ECRG2) was loaded on the column for cleavage of the Trx fusion protein, and the solution in the column was circulated by a pump for 16 h at room temperature. Afterwards, the column was washed again with 50 ml of the buffer A. The ECRG2 containing fractions were concentrated to 5 ml by an ultrafiltration. The collected solution was loaded onto a Superdex 50 column pre-equilibrated with 0.1 mM NH_4HCO_3 buffer. Then the column was washed with 0.1 mM NH_4HCO_3 buffer. The collected fraction containing ECRG2 was lyophilized. Eluted fraction of protein was >99% pure as verified by SDS–PAGE. To substantiate the identity of purified ECRG2, mass spectrum was recorded on an Applied Biosystems Voyager MALDI-TOF mass spectrometer.

Uniformly ^{15}N- and ^{13}C-single labeled and $^{15}N/^{13}C$-double labeled ECRG2 were obtained by growth in minimal media containing $^{15}NH_4Cl$ and/or [^{13}C]-glucose as the sole nitrogen and/or carbon sources. The purity of proteins was checked by SDS–PAGE to ensure a single band.

NMR spectroscopy

The NMR samples contained 1.0 mM ^{15}N-, ^{13}C-, or $^{15}N/^{13}C$-labeled ECRG2, 100 mM KCl, and 0.01% NaN_3 in 50 mM deuterated acetate buffer (pH 5.0). All NMR experiments were run on a Bruker DMX 600 MHz spectrometer equipped with a triple-resonance cryo-probe at 293 K. The 2D $^1H–^{15}N$ HSQC and 3D $^1H–^{15}N–^{13}C$ HNCO, HNCA, HN(CO)CA, HN(CA)CO, HNCACB, CBCA(CO)NH, and HBHA(CO)NH, and 3D $^1H–^{15}N$ TOCSY-HSQC and NOESY-HSQC experiments were adopted for the resonance assignments. All NMR data were processed and analyzed with FELIX software (Accelrys Inc.). ^1H chemical shifts were referenced to the internal DSS (2,2-dimethyl-2-silaentane-5-sulphonate). ^{15}N chemical shifts were referenced indirectly [11].

Results

Recombinant ECRG2 for NMR experiments

In this study, the stable-isotope-labeled ECRG2 is required for analysis the interaction of ECRG2 with uPA. Hence, the pET-32a-Trx-(linker-Xa)-ECRG2 expression plasmid was obtained, and the desired fusion protein Trx-(linker-Xa)-ECRG2 was expressed in the soluble form. As is well known, missing or wrong disulfide bridges often cause formation of insoluble aggregates when extracellular proteins containing cysteine residues are expressed in the conventional *E. coli* strains [12]. However, using *E. coli* Origami (DE3) strain which carries a trxB-/gor522-double mutation in the expression of the putative serine proteinase inhibitor allows disulfide formation in its oxidative cytoplasm [13,14]. Actually, expression of ECRG2 in the oxidative cytoplasm of *E. coli* Origami (DE3) provided a soluble form of the protein which can provide a properly folded ECRG2.

Moreover, the constructed plasmid and the expression and purification procedures can facilitate folding of ECRG2 with the correctly formed disulfide bonds. In the fusion protein Trx-(linker-Xa)-ECRG2, there is a linker peptide containing SGSGSGSGSG and a factor Xa cleavage site. This linker peptide makes a relatively large space between the two proteins, facilitating the proper folding of ECRG2 in the fusion protein and the proper cleavage of ECRG2 from the fusion protein using factor Xa. Factor Xa is a proteinase cleaving the fusion protein without the additional amino acid at the N-terminus of the target protein. Thus, the recombinant ECRG2 contains 66 residues (Ser20-Cys85) (Fig. 1). The mass of ECRG2 determined by MALDI-TOF MS analysis is 7192.77 (SM Fig. 2).

A recent report [15] has proposed that the ^{13}C chemical shifts can predict disulfide formation, providing simple rules for predict-

ing the redox state of cysteines. As was indicated, if the $^{13}C_\beta$ chemical shift is greater than 35.0 ppm, the redox state can be assigned to oxidized. The assignment of ECRG2 provided the $^{13}C_\alpha$ and $^{13}C_\beta$ chemical shifts of residues Cys32 ($^{13}C_\alpha$: 53.47 ppm, $^{13}C_\beta$: 40.14 ppm), Cys45 ($^{13}C_\alpha$: 56.55 ppm, $^{13}C_\beta$: 39.10 ppm), Cys53 ($^{13}C_\alpha$: 54.56 ppm, $^{13}C_\beta$: 39.35 ppm), Cys64 ($^{13}C_\alpha$: 60.19 ppm, $^{13}C_\beta$: 35.44 ppm), Cus67 ($^{13}C_\alpha$: 56.25 ppm, $^{13}C_\beta$: 35.19 ppm), and Cys85 ($^{13}C_\alpha$: 56.35 ppm, $^{13}C_\beta$: 38.81 ppm). Apparently, all six cysteines have the $^{13}C_\beta$ chemical shifts larger than 35.0 ppm. Therefore, the recombinant ECRG2 can folded properly with correctly formed disulfide bonds, namely Cys32-Cys67, Cys45-Cys64, and Cys53-Cys85, as indicated in Fig. 1.

Secondary structures of ECRG2

The conformation of ECRG2 was explored by the far-UV CD spectrum (see Supplementary material). Analysis of the CD spectrum of ECRG2 (SM Fig. 3) provided the estimation of the secondary structural components: 14% of α-helix, 29% of β-sheet, 22% of turn, and 34% of loop or coil contents. The consensus chemical shift index (CSI) of ECRG2 (SM Fig. 4) predicts that residues Cys64-Lys72 can form an α-helix and residues Gly75-Arg76-Val77 may form a turn in ECRG2, whereas residues Leu50-Gly54 exhibit the high tendency for forming β-strand. On the other hand, inspection of the NOE data for ECRG2 has found out the ^1H_N–^1H_N NOEs of pairs of residues Gly54-Ile58 and Val52-Tyr60 (Fig. 2A and B). This suggested strongly that two segments of residues Leu50-Gly54 and Ile58-Gly61 must run antiparallel to each other. Moreover, the strong ^1H_N–^1H_N NOEs for pairs of residues: Gly54-Ser55, Ser55-Asp56, Asp56-Tyr57, Asp56-Ile58, and Tyr57-Ile58 as well as weak ^1H_N–^1H_N NOEs of Gly54-Tyr57, Ser55-Tyr57, and Ser55-Ile58 (Fig. 2C) were found in the segment Gly54-Ile58. This means residues Gly54-Ser55-Asp56-Tyr57-Ile58 may form an α-helical turn in the segment Leu50-Gly61, since the segment Leu50-Gly54 has high preference for forming a β-strand. Therefore, the segment Leu50-Gly61 can form an antiparallel β-sheet structure. The closely packing of the C-terminal segment Phe79-Asp82 to the segment Leu50-Gly61 in ECRG2 was indicated by the strong ^1H_N–^1H_N NOE of Cys53-His81, middle NOE of Ser55-Leu80, weak NOEs of Ser55-His81 and Cys53-Leu80 as well as very weak NOEs of Gly54-Leu80 and Gly54-His81. This suggested that segment Phe79-Asp82 runs roughly antiparallel to the segment Pro51-Gly54. The above determined NOE connectivities predicting an antiparallel β-sheet consisting of residues Leu50-Gly61 and Phe79-Asp82 are summarized in Fig. 3.

Therefore, the secondary structural elements in ECRG2 were predicted by comprehensive analysis of the NOE and CD data as well as consensus CSI. ECRG2 may have an α-helix of residues Cys64-Lys72, a turn around residues Asn74-Gly75-Arg76-Val77 on the C-terminal side of the α-helix, and an antiparallel β-sheet consisting of strands Ile58-Gly61 and Leu50-Gly54 with a turn Gly54-Ser55-Asp56-Tyr57-Ile58. The C-terminal segment Phe79-Asp82 may run antiparallel to the β-strand Leu50-Gly54.

Binding of ECRG2 with uPA protein

The recombinant ECRG2 contains five proline residues. Thus, 61 residues were considered in the analysis of interaction between ECRG2 and uPA protein using 2D ^1H–^{15}N HSQC spectrum of ^{15}N-labeled ECRG2 (Fig. 4A). The distribution of amide resonances in Fig. 4A represents a native folded conformation of the recombinant ECRG2. About 92% amide resonances were assigned. There are two sets of cross peaks in Fig. 4, one is strong and the other is weak. The set of strong peaks is from correctly folded ECRG2 whereas the set of sharp unassigned peaks can be considered as resonance signals from species of recombinant ECRG2 with mis-pairing disulfide

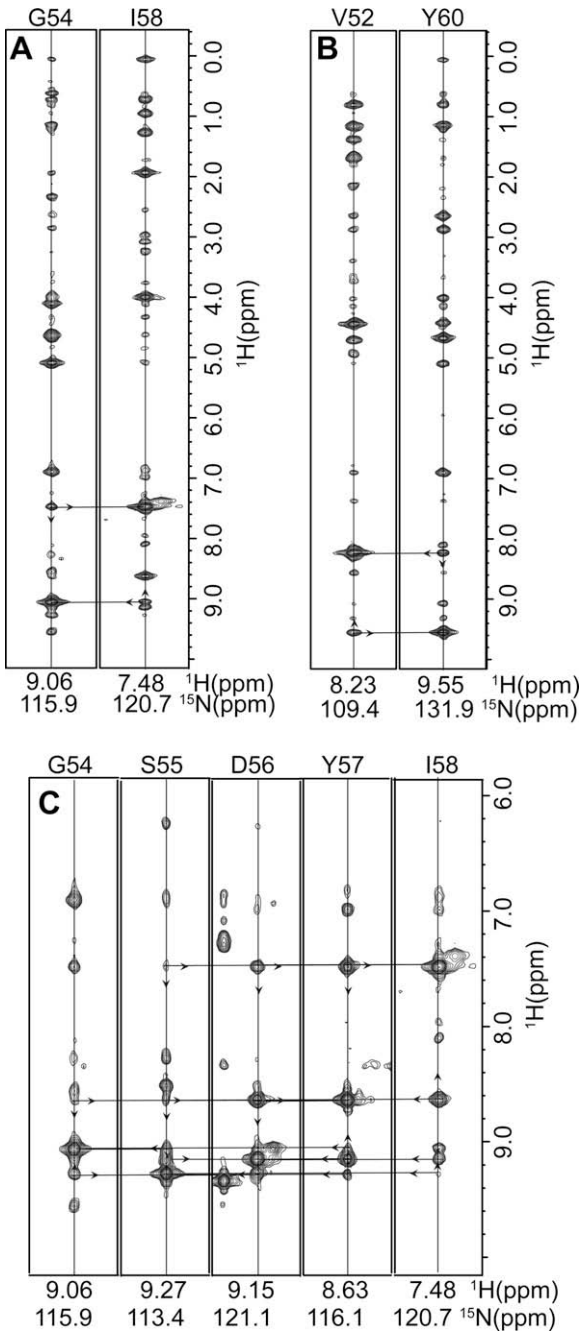

Fig. 2. The ^1H_N–^1H_N NOE connectivities in segment Leu50-Gly61 of ECRG2. NOEs of the pairs of residues Gly54-Ile58 (A) and Val52-Tyr60 (B) between two antiparallel segments Leu50-Gly54 and Ile58-Gly61. (C) NOEs in the segment Gly54-Ile58.

bonds. The intensity ratio of two cross peaks for Gly75 can be used for quantitatively estimating the amount of correctly folded ECRG2 in the sample solution. The estimation of the volumes of two cross peaks for Gly75 provided 83.75% and 16.25% for strong and weak cross peaks, respectively. Since the sample solution used for 2D ^1H–^{15}N HSQC NMR experiments contains total of 0.5 mM ECRG2, the amount of correctly folded ECRG2 is estimated to be 0.42 mM.

Binding of uPA protein with ECRG2 was detected using 2D ^1H–^{15}N HSQC spectrum. Cross peaks in the 2D HSQC spectrum may shift upon the binding of ECRG2 with uPA protein. Fig. 4B shows the spectrum obtained for 0.5 mM ^{15}N-labeled ECRG2 in the presence of 0.5 mM uPA (LIVZON Pharmaceutical Group, Inc., China) (ECRG2 to uPA = 1:1). Clearly, the fast exchange between

Fig. 3. Summary of NOE connectivities predicting an antiparallel β-sheet consisting of residues Leu50-Gly61 and Phe79-Asp82 in ECRG2. The d_{NN} NOE connectivities are indicated by bars connecting the two coupled residues.

resonances for bound and free proteins was observed, suggesting a weak binding affinity. The cross peaks for residues in the sequence regions Val41-Ile43, Ile47-Tyr49, and Tyr60-His65 as well as Val52, Cys67, and Glu69 showed explicit shifts. Of them, the cross peaks for residues Ala42, Ile47, Glu63, Cys64, and Cys67 shifted largely. However, the cross peaks for residues Glu21, Ala23-Leu25, Lys28-Lys29, Asp31-Ser33, Tyr35, Lys37-Tyr38, Leu50, Cys53-Thr59, Thr68, Leu71-Gly75, Val77, Phe79-His81, and Gly83-Ser84 did not shift or showed very little shift. This suggested that the residues in the sequence regions Val41-Ile43, Ile47-Tyr49, and Tyr60-His65 of ECRG2 must be in contact with uPA protein.

When 1 mM uPA (ECRG2 to uPA = 1:2) was added into the ECRG2 sample, vast majority cross peaks in the 2D $^{1}H–^{15}N$ HSQC spectrum were disappeared, only the set of sharp unassigned resonances in Fig 4A and a few strong resonances were remained (Fig. 4C). This can be explained by the fact of binding between ECRG2 and uPA. Due to a higher molecular weight of uPA, the binding of uPA to ECRG2 may cause the formation of a larger protein complex, resulting in the disappearance of the resonances for ECRG2 in the complex with uPA. The remaining sharp unassigned resonances (Fig. 4C) indicate that ECRG2 with mis-pairing disulfide bonds did not interact with uPA. On the other hand, this corroborated that only the species of ECRG2 with correctly formed disulfide bonds can bind to uPA. Nevertheless, the binding of uPA to ECRG2 is weak as indicated above. It should be mentioned that chemical shift changes can also arise from conformational changes, but since the residues showing resonance shifting are much localized (and since all peaks disappear on binding) this is less likely. Thus, the segments Val41-Ile43, Ile47-Tyr49, and Tyr60-His65 form a putative binding site of uPA on ECRG2.

Discussion

Structural resemblance between ECRG2 and OMTKY3

Turkey ovomucoid third domain (OMTKY3) is a canonical inhibitor of serine proteinase which belongs to the Kazal family of proteinase inhibitors [16]. OMTKY3 is a 56-residue polypeptide, which contains three covalent disulfide bonds. The sequence alignment (Fig. 5A) shows that ECRG2 has 40% sequence homologous to OMTKY3. The solution structure of OMTKY3 has been determined (pdb ID: 1TUR), showing one α-helix (Asn33-Ser44), one antiparallel β-sheet constructed by three β-strands (Arg21-Ser26, Lys29-Gly32, and Thr49-Gly54), and four reverse turns: Cys8-Tyr11, Gly25-Asn28, Val42-Asn45, and Ser44-Leu47. Six cysteine residues in the Kazal motif form three pairs of disulfide bonds: Cys8-Cys38, Cys16-Cys35, and Cys24-Cys56 (Fig. 1) [17]. Residues Lys13-Arg21 and Gly32-Asn33 as well as Asn36 in OMTKY3 are in the consensus region of contact with serine proteinases. The reactive site peptide bond is Leu18-Glu19 [18].

Based on the reported 3D structure of OMTKY3, the estimated secondary structure content of OMTKY3 contains approximately 21% α-helix, 29% β-sheet, and 16% turn. These values are in close proximity to the above estimated contents of secondary structural components for ECRG2. The consensus CSI and NOE connectivities (SM Fig. 4 and Figs. 2 and 3) further indicated that the predicted secondary structural regions in ECRG2 are in correspondence with the secondary structural regions in OMTKY3 (Fig. 5A). Therefore, it can be proposed that the 3D structure of ECRG2 resembles those of OMTKY3. The structure of ECRG2 was modeled by software Modeller [19] using OMTKY3 as a template, having an OMTKY3-like tertiary folding (Fig. 5B).

Interaction of uPA protein with ECRG2

As was indicated, Kazal-type proteinase inhibitors bind tightly to their cognate enzymes because their reactive site loops are geometrically complementary to the enzyme active sites [20,21]. OMTKY3 inhibits those serine proteinases that have the chymotryptic specificity. Several groups have reported the binding of OMTKY3 to a bacterial serine proteinase, streptomyces griseus pro-

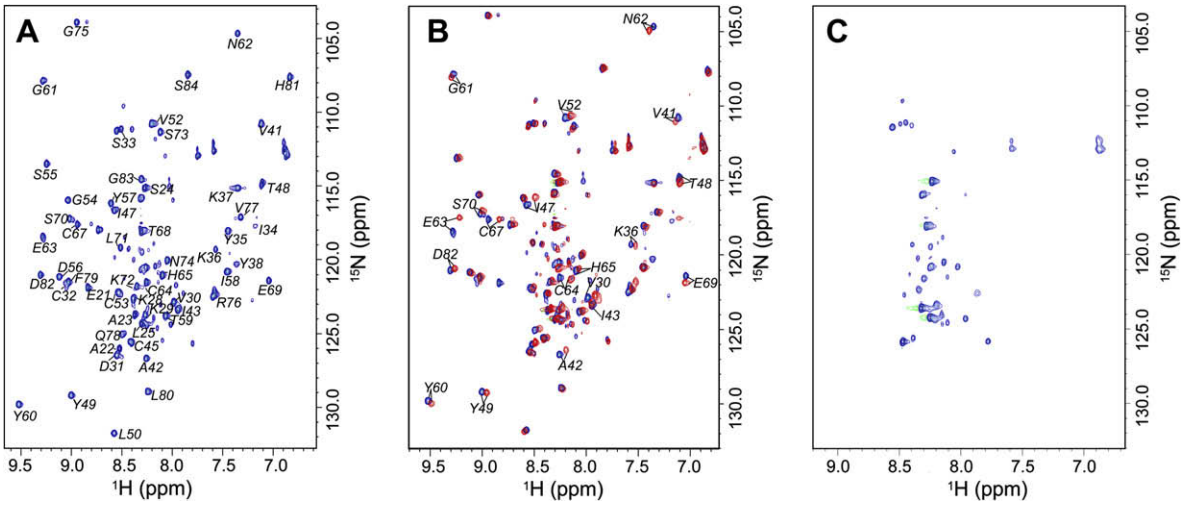

Fig. 4. The binding site of uPA protein on ECRG2. (A) 2D $^{1}H–^{15}N$ HSQC spectrum of ECRG2 showing the residue-specific assignments of backbone amide groups. The assigned residues are indicated by labeling the one-letter amino acid code and residue number. (B) The 2D $^{1}H–^{15}N$ HSQC spectrum of 0.5 mM ECRG2 (blue) is overlaid with the spectrum recorded for sample after adding 0.5 mM uPA protein (ECRG2:uPA = 1:1) (red). (C) The 2D $^{1}H–^{15}N$ HSQC spectrum of ECRG2 after adding 1 mM uPA protein (ECRG2:uPA = 1:2).

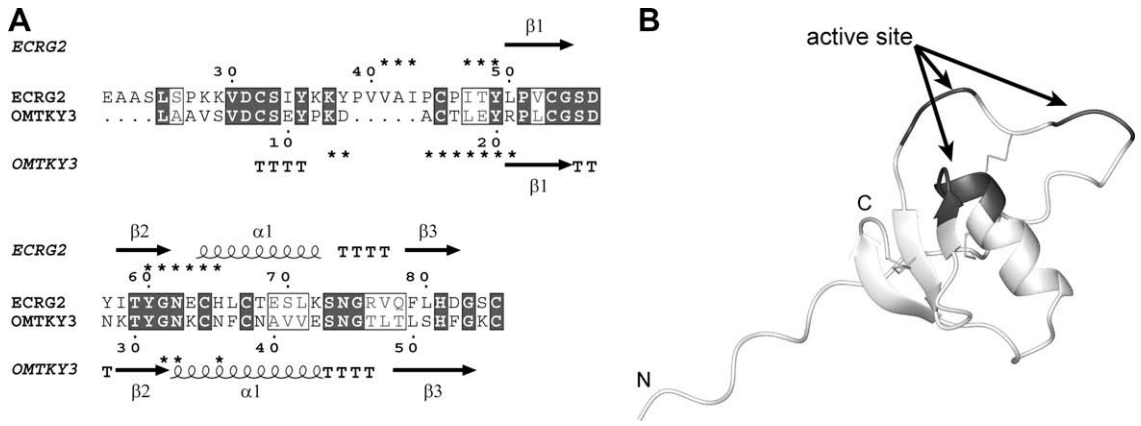

Fig. 5. ECRG2 structure resembles the OMTKY3 structure. (A) Sequence alignment of ECRG2 and OMTKY3. The secondary structural elements and reactive site loops (indicated by star) in OMTKY3 (lower) and the predicted secondary structural elements and putative reactive site loops (indicated by star) of ECRG2 (upper) are shown. (B) Representative structure of ECRG2 generated by homology modeling using OMTKY3 as template. Arrowheads indicate the uPA-binding site in ECRG2 structure.

teinase B (SGPB), and the structure determination showed that OMTKY3 binds tightly to the active site of SGRB [22,23]. Similar to the interaction of OMTKY3 with serine proteinase, uPA exhibited binding to ECRG2 in serum-free conditioned medium from either PG/pcDNA3.1-ECRG2 cells or PG/pcDNA3.1 [10]. As is well known, uPA is a trypsin-like serine proteinase involved in tissue remodeling and cell migration, and inhibits aggressiveness of cancer cell, possibly through the down-regulation of uPA/plasmin activity [24,25]. The molecule of uPA comprises three domains: an N-terminal growth factor domain (GFD), a kringle domain (KD), and a serine proteinase domain. The serine proteinase domain contains the catalytic site [25,26].

In the binding of OMTKY3 with serine proteinase, the active site of serine proteinase binds to the reactive site loops Lys13-Arg21 and Gly32-Asn36 of OMTKY3 [18]. Analysis of the NMR data indicated that segments of residues Val41-Ile43, Ile47-Tyr49, and Tyr60-His65 of ECRG2 are the uPA-binding regions. The sequence locations of these binding regions in ECRG2 are very similar to those of the reactive site loops in OMTKY3 (Fig. 5A and B). In other words, the sequence regions for binding of uPA protein in ECRG2 are in correspondence with the reactive site loops for binding of serine proteinase in OMTKY3. Apparently, segments Val41-Ile43, Ile47-Tyr49, and Tyr60-His65 can be considered as the putative reactive site loops for uPA binding in ECRG2. Therefore, similar to the binding of OMYKY3 with serine proteinase, ECRG2 can bind with serine proteinase domain of uPA. However, the present research can not provide the information about the binding site on the serine proteinase domain of uPA. This requires the further study of the interaction between ECRG2 and serine proteinase domain of uPA, and determination of the complex structure of ECRG2 with the serine proteinase domain of uPA protein.

In conclusion, the expression of ECRG2 in the oxidative cytoplasm of *E. coli* Origami (DE3) resulted in soluble, properly folded protein with accurately formed disulfide bonds. The structural similarity of ECRG2 to OMTKY3 was identified. The experimentally determined putative reactive site loops for binding of uPA in ECRG2 are in correspondence with the reactive site loops for binding of serine proteinase in OMTKY3.

Acknowledgment

This research was supported by the National Natural Science Foundation of China (NNSFC 30770434).

Appendix A. Supplementary data

Supplementary data associated with this article can be found, in the online version, at doi:10.1016/j.abb.2008.08.023.

References

[1] C.M. Yue, M.X. Bi, W. Tan, D.J. Deng, X.Y. Zhang, L.P. Guo, D.X. Lin, S.H. Lu, Int. J. Cancer 108 (2004) 232–236.
[2] Y.P. Cui, J.B. Wang, X.Y. Zhang, R.G. Lang, M.X. Bi, L.P. Guo, S.H. Lu, Biochem. Biophys. Res. Commun. 302 (2003) 904–915.
[3] C.O. Simpkins, Cell. Mol. Biol. 46 (2000) 465–488.
[4] R.X. Jin, B.H. Bay, V.T.K. Chow, P.H. Tan, T. Dheen, Cell Tissue Res. 303 (2001) 221–226.
[5] Y.P. Cui, J.B. Wang, X.Y. Zhang, M.X. Bi, L.P. Guo, S.H. Lu, World J. Gastroenterol. 9 (2003) 1892–1896.
[6] C. Takahashi, Z.Q. Sheng, T.P. Horan, H. Kitayama, M. Maki, K. Hitomi, Y. Kitaura, S. Takai, R.M. Sasahara, A. Horimoto, Y. Ikawa, B.J. Ratzkin, T. Arakawa, M. Noda, Proc. Natl. Acad. Sci. USA 95 (1998) 13221–13226.
[7] J. Oh, R. Takahashi, S. Kondo, A. Mizoguchi, E. Adachi, R.M. Sasahara, S. Nishimura, Y. Imamura, H. Kitayama, D.B. Alexander, C. Ide, T.P. Horan, T. Arakawa, H. Yoshida, S.I. Nishikawa, Y. Itoh, M. Seiki, S. Itohara, C. Takahashi, M. Noda, Cell 107 (2001) 789–800.
[8] L.T. Liu, H.C. Chang, L.C. Chiang, W.C. Hung, Cancer Res. 63 (2003) 3069–3072.
[9] M.L. Huhtala, K. Pesonen, N. Kalkkinen, U.H. Stenman, J. Biol. Chem. 257 (1982) 13713–13716.
[10] G. Huang, Z. Hu, M. Li, Y. Cui, Y. Li, L. Guo, W. Jiang, S.H. Lu, Carcinogenesis 28 (2007) 2274–2281.
[11] J.L. Markley, A. Bax, Y. Arata, C.W. Hilbers, R. Kaptein, B.D. Sykes, P.E. Wright, K. Wuthrich, Pure Appl. Chem. 70 (1998) 117–142.
[12] A. Mitraki, J. King, Nat. Biotechnol. 7 (1989) 690–697.
[13] A.I. Derman, W.A. Prinz, D. Belin, J. Beckwith, Science 262 (1993) 1744–1747.
[14] W.A. Prinz, F. Aslund, A. Holmgren, J. Beckwith, J. Biol. Chem. 272 (1997) 15661–15667.
[15] D. Sharma, K. Rajarathnam, J. Biomol. NMR 18 (2000) 165–171.
[16] M. Laskowski Jr., I. Kato, Annu. Rev. Biochem. 49 (1980) 593–626.
[17] A.M. Krezel, P. Darba, A.D. Robertson, J. Fejzo, S. Macura, J.L. Markley, J. Mol. Biol. 242 (1994) 203–214.
[18] J.K. Song, M. Laskowski, M.A. Qasim, J.L. Markley, Biochemistry 42 (2003) 6380–6391.
[19] A. Sali, T.L. Blundell, J. Mol. Biol. 234 (1993) 779–815.
[20] R.J. Read, M. James, Introduction to the protein inhibitors: X-ray crystallography, in: A. Barrett, G. Salvesen (Eds.), Proteinase Inhibitors, Elsevier Science Publishers B.V., Amsterdam, 1986, pp. 301–336.
[21] W. Bode, R. Huber, Eur. J. Biochem. 204 (1992) 433–451.
[22] M. Fujinaga, R.J. Read, A. Sielecki, W. Ardelt, M. Laskowski Jr., M.N. James, Proc. Natl. Acad. Sci. USA 79 (1982) 4868–4872.
[23] K.S. Bateman, S. Anderson, W.Y. Lu, M.A. Qasim, M. Laskowski, M.N.G. James, Protein Sci. 9 (2000) 83–94.
[24] M.P. Crippa, Int. J. Biochem. Cell Biol. 39 (2007) 690–694.
[25] E. Zeslawska, J. Sturzebecherb, B.J. Oleksyn, Med. Chem. Lett. 17 (2007) 6212–6215.
[26] C. Barinka, G. Parry, J. Callahan, D.E. Shaw, A. Kuo, K. Bdeir, D.B. Cines, A. Mazar, J. Lubkowski, J. Mol. Biol. 363 (2006) 482–495.